

This document is confidential and is proprietary to the American Chemical Society and its authors. Do not copy or disclose without written permission. If you have received this item in error, notify the sender and delete all copies.

**Self-Assembly Behavior of Alkylated Isophthalic Acids
Revisited: Concentration in Control and Guest Induced
Phase Transformation**

Journal:	<i>Langmuir</i>
Manuscript ID:	la-2014-040849.R1
Manuscript Type:	Article
Date Submitted by the Author:	24-Nov-2014
Complete List of Authors:	Park, Kwang-Won; Chung-Ang University, Department of Chemistry Adisoejoso, Jinne; KU Leuven, Department of Chemistry Plas, Jan; KU Leuven, Department of Chemistry Hong, Jongin; Chung-Ang University, Chemistry Müllen, Klaus; Max-Planck-Institute for Polymer Research, De Feyter, Steven; KU Leuven, Department of Chemistry

SCHOLARONE™
Manuscripts

1
2
3
4 **Self-Assembly Behavior of Alkylated Isophthalic Acids Revisited:**
5
6
7 **Concentration in Control and Guest Induced Phase**
8
9
10 **Transformation**
11
12
13
14

15 Kwang-Won Park^{1,2}, Jinne Adisoejoso^{1*}, Jan Plas¹, Jongin Hong², Klaus Müllen³, Steven De Feyter^{1*}
16
17
18
19
20
21
22

23 1. Division of Molecular Imaging and Photonics, Department of Chemistry, KU Leuven,
24 Celestijnenlaan 200 F, 3001 Leuven, Belgium.
25
26

27 2. Department of Chemistry, Laboratory of Nano-material Chemistry, Chung-Ang University, Seoul
28 156-756, Republic of Korea
29
30

31 3. Max-Planck Institute for Polymer Research, Ackermannweg 10, D-55128, Mainz, Germany.
32
33
34
35
36

37 Key words: phase behavior, host-guest systems, concentration control, scanning tunneling microscopy,
38 self-assembly
39
40
41
42
43

44 **Abstract**

45
46

47 The engineering of two-dimensional crystals by physisorption-based molecular self-assembly at the
48 liquid-solid interface is a powerful method to functionalize and nanostructure surfaces. Formation of
49 high symmetry networks from low symmetry building blocks is a particularly important target.
50
51 Alkylated isophthalic acid (ISA) derivatives are early test systems, and it was demonstrated that in
52 order to produce a so-called porous hexagonal packing of plane group $p6$, i.e. a regular array of
53 nanowells, either short alkyl chains or the introduction of bulky groups within the chains were
54
55
56
57
58
59
60

1
2
3 mandatory. After all, the van der Waals interactions between adjacent alkyl chains or alkyl chains and
4
5 the surface would dominate the ideal hydrogen bonding between the carboxyl groups and therefore a
6
7 close packed lamella structure (plane group $p2$) was uniquely observed. In this contribution, we show
8
9 two versatile approaches to circumvent this problem, which are based on well-known principles: the
10
11 “concentration in control” and the “guest induced transformation” method. The successful application
12
13 of these methods makes ISA suitable building blocks to engineer a porous pattern in which the distance
14
15 between the pores can be tuned with nanometer precision.
16
17
18
19
20
21

22 Introduction

23
24
25
26
27

28 Surface confined two-dimensional (2D) crystals consisting of molecular building blocks have garnered
29
30 a broad interest in nanoscience due to their potential applications.^{1, 2, 3, 4} Traditionally, non-covalent
31
32 interactions are used to guide the self-assembly process. By using hydrogen bonding^{5, 6, 7, 8}, van der
33
34 Waals interactions^{9, 10, 11, 12}, metal-ligand coordination^{13, 14, 15} or a combination thereof as a molecular
35
36 ‘glue’, a multitude of architectures have been successfully engineered both in ultra-high vacuum
37
38 conditions as well as at a liquid-solid interface. Predicting the specific outcome of network formation
39
40 based on the molecular building blocks remains a challenge as various experimental factors govern the
41
42 self-assembly process: solute concentration,^{10, 16, 17, 18, 19, 20} temperature^{21, 22, 23, 24, 25}, solvent^{26, 27} have
43
44 all been known to influence the 2D crystal formation under ambient conditions.
45
46
47
48
49
50

51 It has previously been reported that alkylated isophthalic acid derivatives (ISA) show a variety of self-
52
53 assembly motifs at the liquid/highly oriented pyrolytic graphite (HOPG) interface, where the outcome
54
55 is determined by changes of the alkyl chains.^{28, 29, 30} The main driving force for self-assembly was
56
57 expected to be the intermolecular interaction between carboxylic groups in meta position, which, after
58
59
60

1
2
3 dimerization through hydrogen bonding, potentially could yield linear zig-zag or hexameric structures.
4
5
6 It turned out however, that ISA derivatives with a simple linear alkyl chain uniquely formed a lamellar
7
8 structure in which the intermolecular van der Waals interactions between adjacent interdigitated alkyl
9
10 chains as well as the interaction between the chains and the underlying graphite dominate the hydrogen
11
12 bonding. This forces the structure to circumvent ideal hydrogen bond formation. Only by significantly
13
14 reducing the alkyl chain length and thereby lowering the impact of van der Waals interactions in favor
15
16 of hydrogen bonding, cyclic hexameric structures were obtained.²⁹ As an alternative approach, the
17
18 introduction of bulky groups at the end of the alkyl tails which prevent ideal alkyl chain interdigitation
19
20 also produced hexameric structures.²⁸
21
22
23
24
25
26

27 In this work, we show two simple approaches to create 2D nanoporous hexameric patterns at the liquid-
28
29 solid interface using alkylated ISA derivatives without any inherent structural modifications of the
30
31 building blocks, which are based on two well-known principles: “concentration in control”¹⁶ and
32
33 “guest-induced transformation”³¹.
34
35
36
37
38

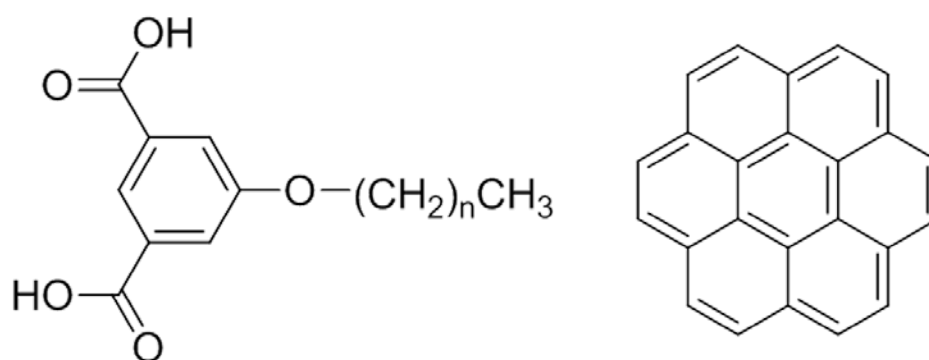
39 **Results & Discussions**

40 41 42 43 44 **1. Concentration in Control**

45
46
47
48
49 Three ISA derivatives (5-decyloxy-isophthalic acid (ISA-OC10), 5-tetradecyloxy-isophthalic acid,
50
51 (ISA-OC14) and 5-octadecyloxy-isophthalic acid (ISA-OC18)) which differ only in the length of the
52
53 alkyl chains were chosen (scheme 1) and their 2D self-assembly behavior at the liquid-solid interface
54
55 was explored by scanning tunneling microscopy (STM). These molecular building blocks have two
56
57 intrinsic recognition sites for non-covalent interactions: the alkyl chains give rise to van der Waals
58
59
60

1
2
3 interactions through interdigitation and the carboxylic acid groups form hydrogen bonds. Depending
4
5 on the solute concentration used, ISA-OC10 as well as -OC14 form a mixture of two distinct
6
7 polymorphs, linear and porous, upon adsorption at the 1-phenyloctane/HOPG interface, while ISA-
8
9 OC18 yields only the linear polymorph (Figure S2,3,4). Figure 1 shows high-resolution STM images
10
11 of the linear and porous polymorphs formed by ISA-OC14. At relatively high concentration, a lamellar
12
13 structure is predominantly observed for all three derivatives, similar to what has been reported earlier.²⁸
14
15
16
17 ²⁹ Within this lamellar structure, the van der Waals interactions clearly dominate the hydrogen bond
18
19 formation and forces the molecules into a close packed $p2$ structure. The aromatic ISA head groups
20
21 appear as bright circles. Based on the STM contrast it was impossible to determine the exact orientation
22
23 or nature of the hydrogen bonds between the ISA head groups; but due to their head-to-head orientation
24
25 (blue line in Figure 1a), dimer formation between the carboxylic acid functionalities can be excluded.³²
26
27 It remains uncertain, however, how the ISA headgroups interact, therefore only tentative models are
28
29 given in Figure 1a and S1. The angle between the lamella axis and the alkyl chains is $90\pm 1^\circ$ for ISA-
30
31 OC18, while for ISA-OC14 ($\alpha=84\pm 1^\circ$ and $\beta=86\pm 1^\circ$, Figure 1a) and ISA-OC10 ($\alpha=78\pm 1^\circ$ and $\beta=86\pm 1^\circ$,
32
33 Figure S1) two distinct orientations are observed. While for ISA-OC18 all alkyl chains are oriented
34
35 parallel to one of main symmetry axes of HOPG, only the alkyl chains following the β angle (between
36
37 lamella axis and the alkyl chains) are parallel to the main symmetry axis of HOPG.³³ This disparity
38
39 can be understood as follows: relatively shorter alkyl chains give rise to a smaller contribution of van
40
41 der Waals interactions to the structure formation and the hydrogen bonds are therefore playing a more
42
43 important role. However; the former still remains the dominant driving force for self-assembly.
44
45
46
47
48
49
50
51
52
53
54
55
56
57
58
59
60
Bernasek *et al* estimated the energy contributions of hydrogen bond formation and van der Waals
interaction in the lamellar structure of ISA-OC10 and ISA-OC18.²⁹ They confirmed that the share of
hydrogen bonds (30-50 kJ/mol for both ISA-OC10 and ISA-OC18) increases as the share of van der
Waals interaction decreases with shorter alkyl chains (108-126 kJ/mol for ISA-OC18 to 60-70 kJ/mol

1
2
3 for ISA-OC10).
4
5
6
7



20
21 Scheme 1. Molecular structure of ISA-OCn molecules (left): n=9 for ISA-OC10, n=13 for ISA-
22
23 OC14, n=17 for ISA-OC18. Molecular structure of coronene (right).
24
25
26
27
28
29
30
31
32
33
34
35
36
37
38
39
40
41
42
43
44
45
46
47
48
49
50
51
52
53
54
55
56
57
58
59
60

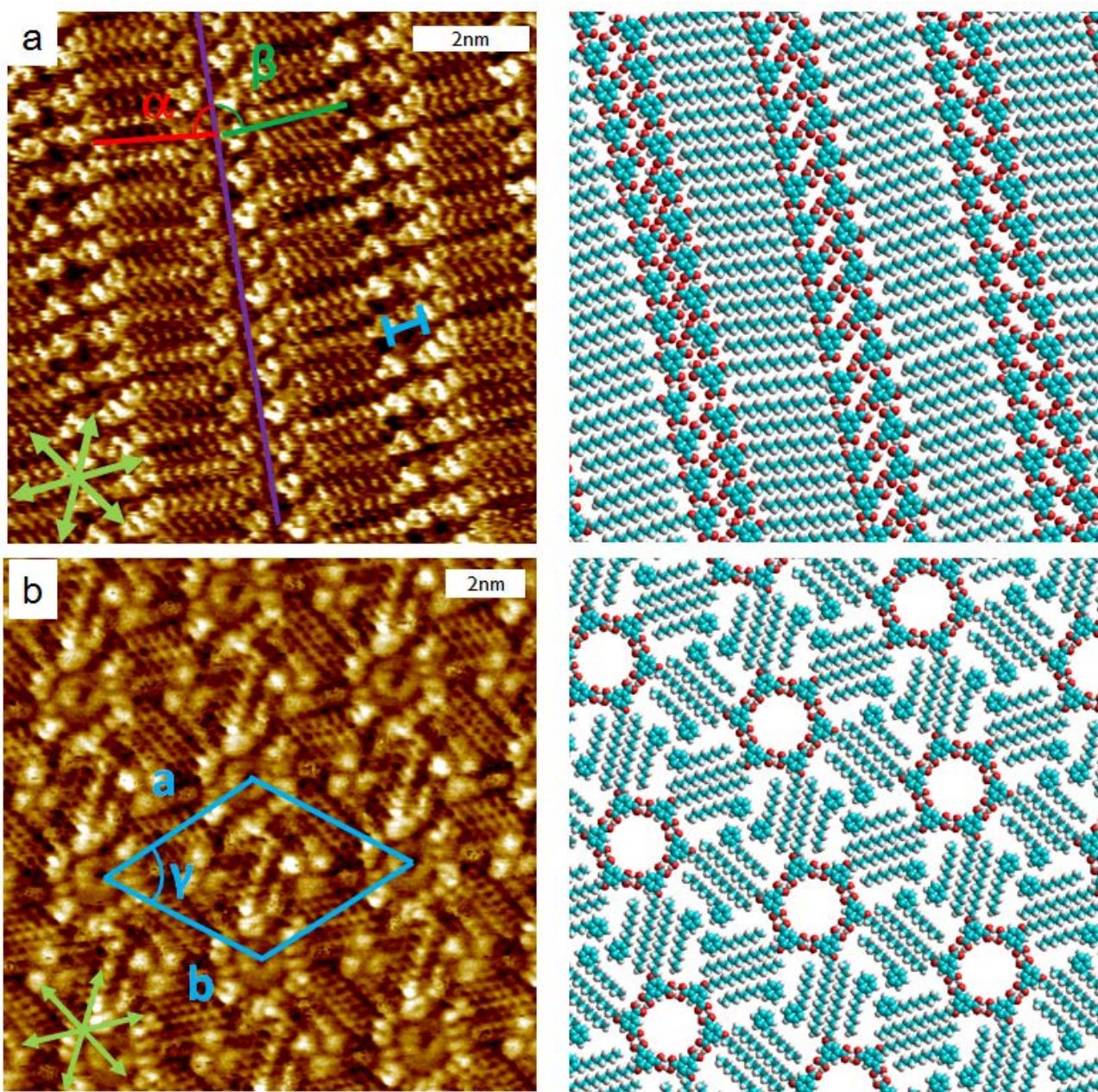


Figure 1. STM images and corresponding tentative molecular models of ISA-OC14 at the 1-phenyloctane / HOPG interface (0.52mM, $V_{\text{bias}} = 0.55$ V, $I_{\text{set}} = 0.13$ nA), showing a) the linear $p2$ network (α and β indicate the angle between the alkyl chains and the lamella axis) and b) The hexameric porous $p6$ phase ($\gamma = 61 \pm 4^\circ$, $a = 4.00 \pm 0.2$ nm, $b = 4.30 \pm 0.1$ nm). The blue line indicates the distance between adjacent aromatic parts of ISA molecules. HOPG lattice vectors are indicated in green.

1
2
3
4
5
6
7
8 Coexisting with the lamellar structure, ISA-OC10 and ISA-OC14 also form a hexameric porous *p6*
9 structure at higher concentration, which is phase separated from the lamellar network. Lowering the
10 solute concentration leads to the unique formation of this hexameric porous structure for ISA-OC10
11 and ISA-OC14 (Figure S1 and 1b, respectively), while the lamellar structure of ISA-OC18 seems to
12 be unaffected by solute concentration: it is still uniquely observed. Unlike the lamellar structure, within
13 the hexameric structure the hydrogen bonding is the dominant intermolecular interaction and the
14 system adapts ideal hydrogen bond formation i.e. the dimer formation between adjacent carboxylic
15 acids as observed previously in case of non-alkylated ISA³⁴ and structurally related trimesic acids³².
16 The hydrogen bonded hexagonal pores are in their turn surrounded by six triangular pores, formed by
17 van der Waals mediated alkyl chain interdigitation. After close inspection, it was found that for ISA-
18 OC14 3 phenyloctane solvent molecules reside in the triangular pores, identified by their bright
19 aromatic headgroups.³⁵ Coadsorption of these solvent molecules compensates for the loss in stability
20 due to the large unoccupied areas in the triangular pores. Within the hexameric structure of ISA-OC10,
21 the triangular pores become too small for solvent coadsorption and appear featureless. This explains
22 why the decrease of the hexameric structure coverage with increasing concentration happens much
23 faster for ISA-OC10 in respect to ISA-OC14. Decreasing the alkyl chain length maintains the
24 hexagonal pore diameter constant (1.13 ± 0.1 nm), while decreasing the area of the triangular pores or
25 in other words decreasing the distance between adjacent hexagonal pores.
26
27
28
29
30
31
32
33
34
35
36
37
38
39
40
41
42
43
44
45
46
47
48
49

50 The dependence of the surface coverage of porous polymorph on the concentration of ISA in solution
51 is shown in Figure 2.³⁶ As can be seen from the graph, for both ISA-OC10 and ISA-OC14, the porous
52 hexameric structure can be homogeneously engineered by using sufficiently low concentration.
53 Surprisingly, even at the lowest concentration probed (0.01 mM) ISA-OC18 still exclusively forms the
54
55
56
57
58
59
60

1
2
3 lamellar network even though the surface coverage becomes sub-monolayer (Figure S4).
4
5
6
7

8 The concentration dependency of ISA derivatives is in good agreement with what has been observed
9
10 earlier with similar molecular building blocks.¹⁶ Traditionally, systems that are sensitive towards
11
12 concentration consist of building blocks which are able to form two or more polymorphs with
13
14 different adsorption energy and/or packing density. For ISA-OC10 and ISA-OC14, the packing density
15
16 of the lamellar structure (1.23 molecules/nm² for ISA-OC10, 0.69 molecules/nm² for ISA-OC14) and
17
18 the hexameric structure (0.48 molecules/nm² for ISA-OC10, 0.33 molecules/nm² for ISA-OC14)
19
20 differs significantly. Therefore at high concentration, the number of molecules exceeds the amount
21
22 required to cover the surface through hexameric structures and the system reacts by forming the close-
23
24 packed lamella structure, by using van der Waals forces between alkyl chains as the dominant driving
25
26 force. However at lower concentration, less molecules are present at the interface and the system will
27
28 react by forming the low density network and allowing hydrogen-bond formation dictating the
29
30 structure. Compared to ISA-OC10 and ISA-OC14, the difference in packing density between lamella
31
32 and hexamers of ISA-OC18 is even larger. However, the energy penalty induced by the uncovered area
33
34 of the triangular pores is simply too large and therefore, even at sub-monolayer coverage, the formation
35
36 of lamellae of ISA-OC18 is uniquely observed (Figure S4).
37
38
39
40
41
42
43
44
45
46
47
48
49
50
51
52
53
54
55
56
57
58
59
60

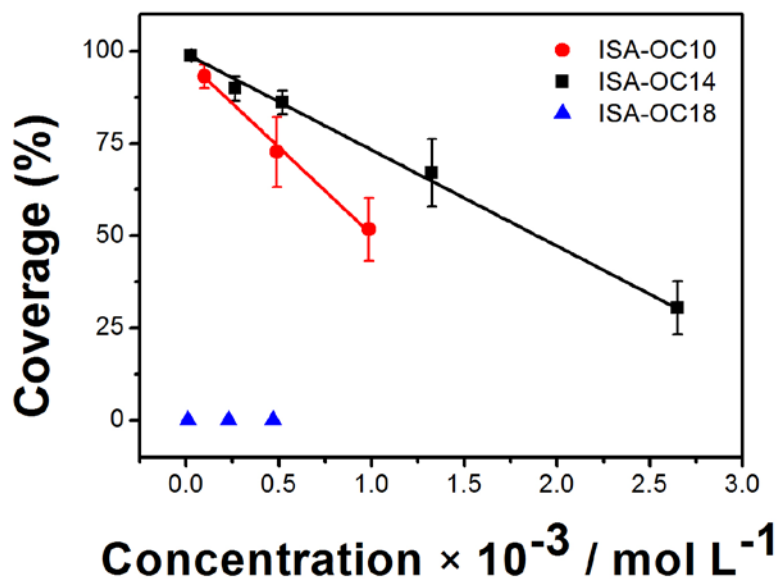


Figure 2. Dependence of the surface coverage of the porous structure on the ISA concentration in solution. For each concentration, typically 10 to 15 large scale images ($100 \text{ nm} \times 100 \text{ nm}$) were recorded at different locations in order to be statistically relevant (Figure S3)

2. Guest induced transformation

One of the main applications for nanoporous systems is the selective trapping of guest molecules in a spatially resolved manner. Moreover, apart from simple coadsorption, it has been well documented that the addition of guest molecules can overcome the energy loss caused by unoccupied areas and thereby templating the formation of a specific network.^{31, 37, 38, 39} As non-alkylated ISA has been successfully applied to host coronene (COR), COR was chosen as guest for the alkylated ISA host-network.³⁴

Upon premixing COR and the alkylated ISA derivatives in a 1:1 molar ratio (COR/ISA-OC10

1
2
3 1mM/0.98mM, COR/ISA-OC14 3mM/2.65mM, COR/ISA-OC18 0.5mM/0.47mM), the hexameric
4 structure is exclusively observed for all the three derivatives (Figure 3a-c). The COR molecules appear
5 as bright circular features within the hexagonal hydrogen-bonded pores of ISA. In the absence of COR,
6 but maintaining the same concentration of the ISA derivatives, the lamellar structure is the dominant
7 polymorph. Therefore, COR not only acts as a guest molecule. Under conditions where ISA forms a
8 lamellar structure, its presence forces the system to transform from a lamellar structure into the
9 hexameric network. After closer inspection, it appears that both for ISA-OC18 and ISA-OC14 (Figure
10 3b-c), the triangular pores are also accommodating COR molecules. In the case of ISA-OC18, the
11 COR molecules inside the triangular pores appear as fuzzy features, while the COR molecules inside
12 the hexagonal void are well resolved, which can be correlated to the size mismatch between the
13 triangular void and the adsorption of 1 COR molecule. Based on molecular modelling, a COR
14 molecule adsorbed inside the triangular pore has the freedom to rotate and translate and the dynamic
15 nature of COR adsorption into size-mismatched pores has been reported previously.¹¹ The COR
16 molecules hosted inside the triangular pores of ISA-OC14, however, appear to be well immobilized
17 and even though the triangular pore does not match the hexagonal shape of the COR molecule, the size
18 matching appears to be sufficient to immobilize COR. In contrast, the presence of COR has a more
19 dramatic effect on the hexameric structure of ISA-OC10. Based on molecular modeling, the triangular
20 pore of ISA-OC10 would be too small for the coadsorption of COR. COR addition, however, changes
21 the hexameric patterns such that within a hexamer of ISA-OC10, four out of six alkyl chains are not
22 interdigitated, thus creating additional empty space for the adsorption of COR. Within a unit cell,
23 besides two triangular pores, each hosting a single COR molecule, a rhombic pore is created which
24 hosts two COR molecules (Figure 3a).

25
26
27
28
29
30
31
32
33
34
35
36
37
38
39
40
41
42
43
44
45
46
47
48
49
50
51
52
53
54
55
56
57
58 As the presence of COR has an impact on the polymorph formation, it is not farfetched that the ratio
59
60

1
2
3 of COR vs ISA could have an impact on the monolayer composition and architecture as well. This
4
5 aspect was explored for ISA-OC10. Lowering the COR/ISA ratio gradually reduces the number of
6
7 COR molecules adsorbed per unit cell. At a COR/ISA molar ratio of 1:10, a hexameric structure where
8
9 all 6 alkyl chains are interdigitated is observed (Figure 4a). However, the alkyl chain interdigitation
10
11 does not involve the whole end-to-end distance of adjacent alkyl chains in order that the triangular
12
13 pore becomes large enough to host a single COR molecule. Finally, lowering the COR/ISA molar ratio
14
15 to 1:100, COR adsorption only occurs in the hexagonal pores while the triangular pores remain vacant
16
17 (Figure 4b) and ideal alkyl chain interdigitation is restored. This illustrates the flexibility induced by
18
19 the non-covalent van der Waals interactions: the ISA network reacts by expanding its pores to
20
21 accommodate more COR, depending on the specific COR/ISA ratio. This is reflected by the unit cell
22
23 area which increases from 10.9 nm² (1 COR molecules / unit cell) over 11.4 nm² (3 COR molecules /
24
25 unit cell) to 14.0 nm² (5 COR molecules / unit cell) at COR/ISA ratios of 1:100, 1:10 and 1:1
26
27 respectively.
28
29
30
31
32
33
34
35
36
37
38
39
40
41
42
43
44
45
46
47
48
49
50
51
52
53
54
55
56
57
58
59
60

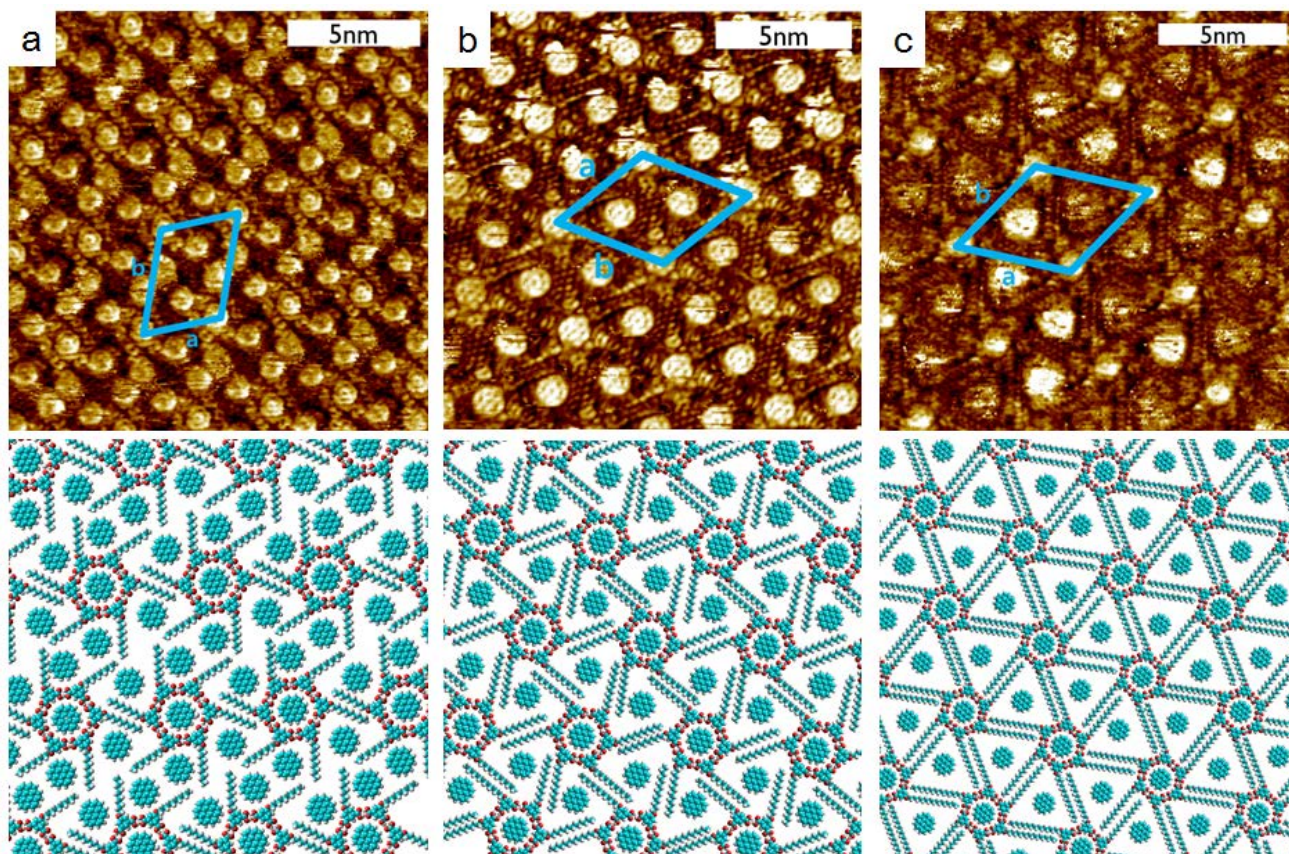


Figure 3: STM images and corresponding tentative models of a mixture of COR and a) ISA-OC10, b) ISA-OC14 and c) ISA-OC18 in a 1:1 ratio (COR/ISA-OC10 1mM/0.98mM, COR/ISA-OC14 3mM/2.65mM, COR/ISA-OC18 0.5mM/0.47mM) Unit cell parameters are a) $\alpha = 68.6 \pm 1.3^\circ$, $a = 3.24 \pm 0.1$ nm, $b = 4.64 \pm 0.3$ nm, b) $\alpha = 59.8 \pm 2.5^\circ$, $a = 3.58 \pm 0.1$ nm, $b = 3.66 \pm 0.1$ nm and c) $\alpha = 59.0 \pm 2.1^\circ$, $a = 4.02 \pm 0.1$ nm, $b = 4.18 \pm 0.1$ nm, respectively.

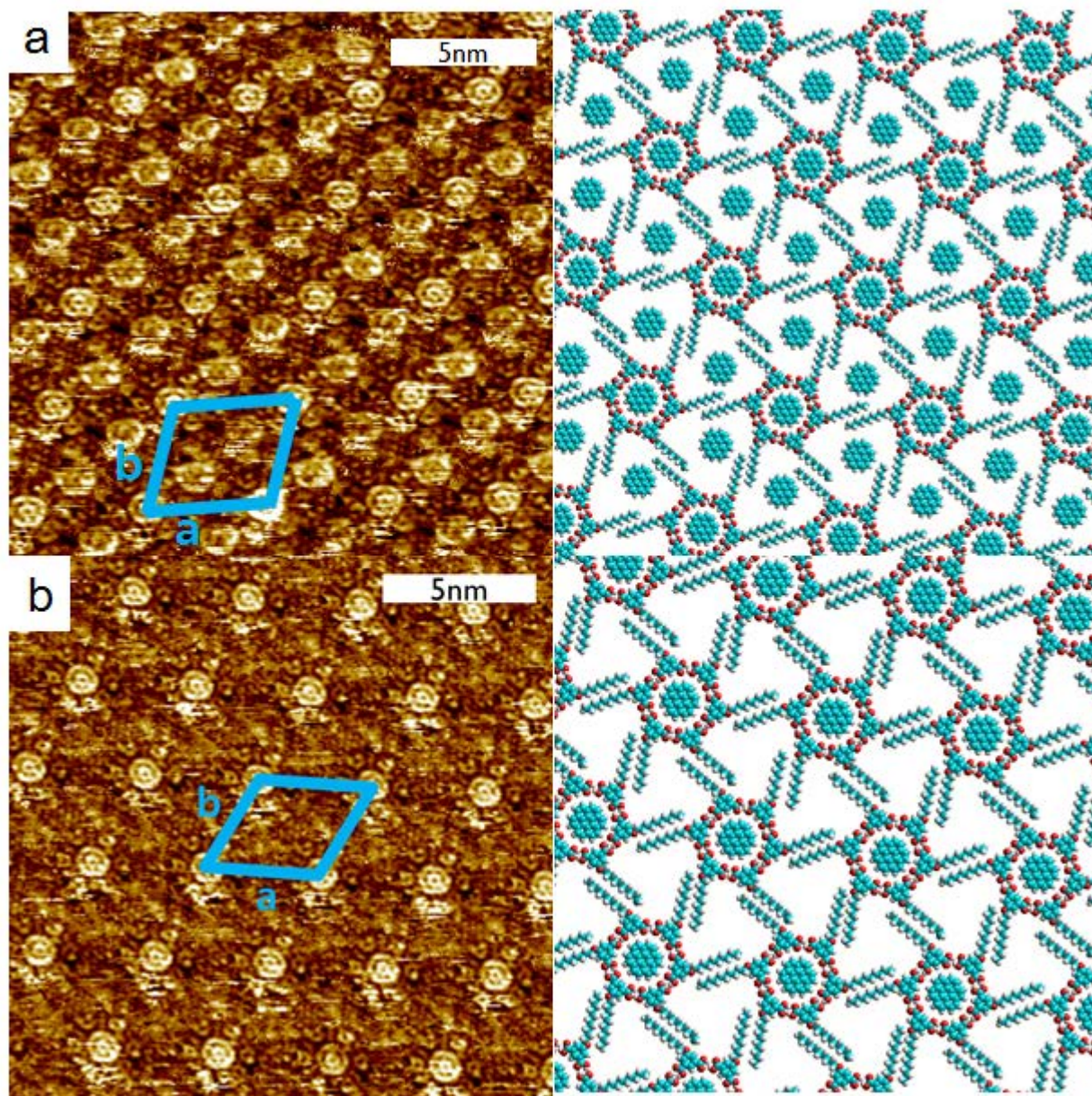


Figure 4: STM images and corresponding tentative molecular models of a premixture of COR and ISA-OC10 at a) 1:10 ratio (COR: 0.10 mM/ ISA-OC10 0.98 mM, $V_{\text{bias}} = -0.65$ V, $I_{\text{set}} = 0.12$ nA) and b) 1:100 ratio (COR: 0.01 mM/ ISA-OC10 0.98 mM, $V_{\text{bias}} = -0.65$ V, $I_{\text{set}} = 0.12$ nA) (Unit cell parameters are a) $\alpha = 75.6 \pm 1.0^\circ$, $a = 2.94 \pm 0.2$ nm, $b = 4.04 \pm 0.1$ nm and b) $\alpha = 61.7 \pm 0.6^\circ$, $a = 3.67 \pm 0.1$ nm, $b = 3.35 \pm 0.1$ nm).

Conclusion

We have investigated the self-assembly properties of a series of alkylated isophthalic acid derivatives, which are governed by an interplay of van der Waals interactions and hydrogen bonds. These molecular building blocks can form two distinct polymorphs. It appears that the formation of these polymorphs is very sensitive to external variables. We have shown that it is possible to selectively form a specific network by varying the solute concentration, where high concentration favors a high-density lamellar packing and low concentration favors the formation of low-density porous networks. Moreover, we have demonstrated that a coronene molecule is not only a suitable guest molecule to reside in the pores but may also induce a structural transformation from the lamellar packing to the porous network. Through a combination of these approaches alkylated isophthalic acid derivatives become suitable building blocks to engineer a regular two-dimensional nanoporous network in which the distance between the pores can be tuned at will.

Acknowledgment

This work is supported by the Fund of Scientific Research–Flanders (FWO), KU Leuven (GOA 11/003), Belgian Federal Science Policy Office (IAP-7/05). K.-W.P. and J.H. acknowledge the Basic Science Research Program (2013-026989) through the National Research Foundation (NRF) funded by the Ministry of Science, ICT & Future Planning (MSIP) of Korea. J.A. is a postdoctoral fellow of the Fund of Scientific Research–Flanders (FWO). This research has also received funding from the European Research Council under the European Union’s Seventh Framework Programme (FP7/2007-2013)/ERC Grant Agreement No. 340324 as well as from DFG Priority Programme SPP 1459, ERC grant on NANOGRAPH, Graphene Flagship (No. CNECT-ICT-604391), and European Union Projects UPGRADE, GENIUS, and MoQuaS.

Supporting Information Available: Additional STM images of the self-assembly behavior of ISA-OC10 and ISA OC18 with corresponding tentative molecular models. This information is available free of charge via the Internet at <http://pubs.acs.org/>.

1. Ciesielski, A.; Palma, C.-A.; Bonini, M.; Samori, P. Towards Supramolecular Engineering of Functional Nanomaterials: Pre-Programming Multi-Component 2D Self-Assembly at Solid-Liquid Interfaces. *Adv. Mater.* **2010**, *22* (32), 3506-3520.
2. Mali, K. S.; Adisojoso, J.; De Cat, I.; Balandina, T.; Ghijsens, E.; Guo, Z.; Li, M.; Sankara Pillai, M.; Vanderlinden, W.; Xu, H.; De Feyter, S. Physisorption for Self-Assembly of Supramolecular Systems: A Scanning Tunneling Microscopy Perspective. In *Supramolecular Chemistry*, John Wiley & Sons, Ltd, 2012.
3. Barth, J. V. Molecular architectonic on metal surfaces. *Annu Rev Phys Chem* **2007**, *58*, 375-407.
4. Nath, K. G.; Ivasenko, O.; MacLeod, J. M.; Miwa, J. A.; Wuest, J. D.; Nanci, A.; Perepichka, D. F.; Rosei, F. Crystal engineering in two dimensions: An approach to molecular nanopatterning. *J. Phys. Chem. C* **2007**, *111* (45), 16996-17007.
5. Pawin, G.; Wong, K. L.; Kwon, K.-Y.; Bartels, L. A homomolecular porous network at a Cu(111) surface. *Science* **2006**, *313* (5789), 961-962.
6. Kampschulte, L.; Lackinger, M.; Maier, A. K.; Kishore, R. S. K.; Griessl, S.; Schmittel, M.; Heckl, W. M. Solvent induced polymorphism in supramolecular 1,3,5-benzenetribenzoic acid monolayers. *J. Phys. Chem. B* **2006**, *110* (22), 10829-10836.
7. Stohr, M.; Wahl, M.; Galka, C. H.; Riehm, T.; Jung, T. A.; Gade, L. H. Controlling molecular assembly in two dimensions: The concentration dependence of thermally induced 2D aggregation of molecules on a metal surface. *Angew Chem Int Edit* **2005**, *44* (45), 7394-7398.
8. Pawlak, R.; Clair, S.; Oison, V.; Abel, M.; Ourdjini, O.; Zwaneveld, N. A. A.; Gigmes, D.; Bertin, D.; Nony, L.; Porte, L. Robust Supramolecular Network on Ag(111): Hydrogen-Bond Enhancement through Partial Alcohol Dehydrogenation. *Chemphyschem* **2009**, *10* (7), 1032-1035.
9. Xue, Y.; Zimmt, M. B. Patterned Monolayer Self-Assembly Programmed by Side Chain Shape: Four-Component Gratings. *J. Am. Chem. Soc.* **2012**, *134* (10), 4513-4516.
10. Zhang, X.; Chen, T.; Chen, Q.; Deng, G.-J.; Fan, Q.-H.; Wan, L.-J. One Solvent Induces a Series of Structural Transitions in Monodendron Molecular Self-Assembly from Lamellar to Quadrangular to Hexagonal. *Chem. Eur. J.* **2009**, *15* (38), 9669-9673.
11. Schull, G.; Douillard, L.; Fiorini-Debuisschert, C.; Charra, F.; Mathevet, F.; Kreher, D.; Attias, A. J. Selectivity of Single-Molecule Dynamics in 2D Molecular Sieves. *Adv. Mater.* **2006**, *18* (22), 2954-2957.
12. Tahara, K.; Lei, S.; Adisojoso, J.; De Feyter, S.; Tobe, Y. Supramolecular surface-confined architectures created by self-assembly of triangular phenylene-ethynylene macrocycles via van der Waals interaction. *Chem. Commun.* **2010**, *46* (45), 8507-8525.

- 1
2
3
4
5
6
7
8
9
10
11
12
13
14
15
16
17
18
19
20
21
22
23
24
25
26
27
28
29
30
31
32
33
34
35
36
37
38
39
40
41
42
43
44
45
46
47
48
49
50
51
52
53
54
55
56
57
58
59
60
13. Adisojoso, J.; Li, Y.; Liu, J.; Liu, P. N.; Lin, N. Two-Dimensional Metallo-supramolecular Polymerization: Toward Size-Controlled Multi-strand Polymers. *J. Am. Chem. Soc.* **2012**, *134* (45), 18526-18529.
 14. Stepanow, S.; Lingenfelder, M.; Dmitriev, A.; Spillmann, H.; Delvigne, E.; Lin, N.; Deng, X. B.; Cai, C. Z.; Barth, J. V.; Kern, K. Steering molecular organization and host-guest interactions using two-dimensional nanoporous coordination systems. *Nat. Mater.* **2004**, *3* (4), 229-233.
 15. Lingenfelder, M. A.; Spillmann, H.; Dmitriev, A.; Stepanow, S.; Lin, N.; Barth, J. V.; Kern, K. Towards surface-supported supramolecular architectures: tailored coordination assembly of 1,4-benzenedicarboxylate and Fe on Cu(100). *Chem-Eur J* **2004**, *10* (8), 1913-1919.
 16. Lei, S.; Tahara, K.; De Schryver, F. C.; Van der Auweraer, M.; Tobe, Y.; De Feyter, S. One Building Block, Two Different Supramolecular Surface-Confined Patterns: Concentration in Control at the Solid-Liquid Interface. *Angew. Chem. Int. Ed.* **2008**, *47* (16), 2964-2968.
 17. Kampschulte, L.; Werblowsky, T. L.; Kishore, R. S. K.; Schmittel, M.; Heckl, W. M.; Lackinger, M. Thermodynamical Equilibrium of Binary Supramolecular Networks at the Liquid-Solid Interface. *J. Am. Chem. Soc.* **2008**, *130* (26), 8502-8507.
 18. Tahara, K.; Furukawa, S.; Uji-i, H.; Uchino, T.; Ichikawa, T.; Zhang, J.; Mamdouh, W.; Sonoda, M.; De Schryver, F. C.; De Feyter, S.; Tobe, Y. Two-Dimensional Porous Molecular Networks of Dehydrobenzo[12]annulene Derivatives via Alkyl Chain Interdigitation. *J. Am. Chem. Soc.* **2006**, *128* (51), 16613-16625.
 19. Palma, C.-A.; Bonini, M.; Llanes-Pallas, A.; Breiner, T.; Prato, M.; Bonifazi, D.; Samori, P. Pre-programmed bicomponent porous networks at the solid-liquid interface: the low concentration regime. *Chem. Commun.* **2008**, (42), 5289-5291.
 20. Ahn, S.; Matzger, A. J. Six Different Assemblies from One Building Block: Two-Dimensional Crystallization of an Amide Amphiphile. *J. Am. Chem. Soc.* **2010**, *132* (32), 11364-11371.
 21. Blunt, M. O.; Adisojoso, J.; Tahara, K.; Katayama, K.; Van der Auweraer, M.; Tobe, Y.; De Feyter, S. Temperature-Induced Structural Phase Transitions in a Two-Dimensional Self-Assembled Network. *J. Am. Chem. Soc.* **2013**, *135* (32), 12068-12075.
 22. Adisojoso, J.; Tahara, K.; Lei, S.; Szabelski, P.; Rżysko, W.; Inukai, K.; Blunt, M. O.; Tobe, Y.; De Feyter, S. One Building Block, Two Different Nanoporous Self-Assembled Monolayers: A Combined STM and Monte Carlo Study. *ACS Nano* **2011**, *6* (1), 897-903.
 23. Marie, C.; Silly, F.; Torteck, L.; Müllen, K.; Fichou, D. Tuning the Packing Density of 2D Supramolecular Self-Assemblies at the Solid-Liquid Interface Using Variable Temperature. *ACS Nano*. **2010**, *4* (3), 1288-1292.
 24. Gutzler, R.; Sirtl, T.; Dienstmaier, J. r. F.; Mahata, K.; Heckl, W. M.; Schmittel, M.; Lackinger, M. Reversible Phase Transitions in Self-Assembled Monolayers at the Liquid-Solid Interface: Temperature-Controlled Opening and Closing of Nanopores. *J. Am. Chem. Soc.* **2010**, *132* (14), 5084-5090.
 25. Bellec, A.; Arrigoni, C.; Schull, G.; Douillard, L.; Fiorini-Debuisschert, C.; Mathevet, F.; Kreher, D.; Attias, A.-J.; Charra, F. Solution-growth kinetics and thermodynamics of nanoporous self-assembled

1
2
3
4 molecular monolayers. *J. Chem. Phys.* **2011**, *134* (12), 124702-7.

5 26. Yang, Y.; Wang, C. Solvent effects on two-dimensional molecular self-assemblies investigated by
6 using scanning tunneling microscopy. *Curr. Opin. Colloid Int.* **2009**, *14* (2), 135-147.

7 27. Yibao, L.; Zhun, M.; Guicun, Q.; Yanlian, Y.; Qingdao, Z.; Xiaolin, F.; Chen, W.; Wei, H. Solvent effects
8 on supramolecular networks formed by racemic star-shaped oligofluorene studied by scanning tunneling
9 microscopy. *J. Phys. Chem. C* **2008**, *112* (23), 8649-53.

10 28. De Feyter, S.; Gesquière, A.; Klapper, M.; Müllen, K.; De Schryver, F. C. Toward Two-Dimensional
11 Supramolecular Control of Hydrogen-Bonded Arrays: The Case of Isophthalic Acids. *Nano Lett.* **2003**, *3*
12 (11), 1485-1488.

13 29. Dickerson, P. N.; Hibberd, A. M.; Oncel, N.; Bernasek, S. L. Hydrogen-Bonding versus van der
14 Waals Interactions in Self-Assembled Mono layers of Substituted Isophthalic Acids. *Langmuir* **2010**, *26*
15 (23), 18155-18161.

16 30. Bernasek, S. L.; Feng, T. Self-assembly of 5-octadecyloxyisophthalic acid and its coadsorption with
17 terephthalic acid. *Surf. Sci.* **2007**, *601* (10), 2284-90.

18 31. Furukawa, S.; Tahara, K.; De Schryver, F. C.; Van der Auweraer, M.; Tobe, Y.; De Feyter, S. Structural
19 Transformation of a Two-Dimensional Molecular Network in Response to Selective Guest Inclusion. *Angew.*
20 *Chem. Int. Ed.* **2007**, *46* (16), 2831-2834.

21 32. Griessl, S.; Lackinger, M.; Edelwirth, M.; Hietschold, M.; Heckl, W. M. Self-assembled two-
22 dimensional molecular host-guest architectures from trimesic acid. *Single Molecules* **2002**, *3* (1), 25-31.

23 33. These orientations are observed randomly throughout a series of adjacent lamella, therefore unit
24 cell parameters were not calculated.

25 34. Lei, S.; Surin, M.; Tahara, K.; Adisoejoso, J.; Lazzaroni, R.; Tobe, Y.; Feyter, S. D. Programmable
26 Hierarchical Three-Component 2D Assembly at a Liquid-Solid Interface: Recognition, Selection, and
27 Transformation. *Nano Lett.* **2008**, *8* (8), 2541-2546.

28 35. The specific intermolecular interactions between solvent and ISA molecules or mutual solvent
29 molecules at play remains unknown.

30 36. The concentration range probed for ISA-OC10 is limited by its solubility

31 37. Blunt, M. O.; Russell, J. C.; Champness, N. R.; Beton, P. H. Templating molecular adsorption using a
32 covalent organic framework. *Chem. Commun.* **2010**, *46* (38), 7157-7159.

33 38. Li, Y.; Ma, Z.; Deng, K.; Lei, S.; Zeng, Q.; Fan, X.; De Feyter, S.; Huang, W.; Wang, C. Thermodynamic
34 Controlled Hierarchical Assembly of Ternary Supramolecular Networks at the Liquid-Solid Interface. *Chem.*
35 *Eur. J.* **2009**, *15* (22), 5418-5423.

36 39. Lackinger, M.; Heckl, W. M. Carboxylic Acids: Versatile Building Blocks and Mediators for Two-
37 Dimensional Supramolecular Self-Assembly. *Langmuir* **2009**, *25* (19), 11307-11321.

